Conjugated Polymer Photovoltaic Cells

Kevin M. Coakley and Michael D. McGehee*

Department of Materials Science and Engineering, Stanford University, 476 Lomita Mall, Stanford, California 94305-4045

Received March 2, 2004. Revised Manuscript Received June 29, 2004

Conjugated polymers are attractive semiconductors for photovoltaic cells because they are strong absorbers and can be deposited on flexible substrates at low cost. Cells made with a single polymer and two electrodes tend to be inefficient because the photogenerated excitons are usually not split by the built-in electric field, which arises from differences in the electrode work functions. The efficiency can be increased by splitting the excitons at an interface between two semiconductors with offset energy levels. Power conversion efficiencies of almost 4% have been achieved by blending polymers with electron-accepting materials such as C_{60} derivatives, cadmium selenide, and titanium dioxide. We predict that efficiencies higher than 10% can be achieved by optimizing the cell's architecture to promote efficient exciton splitting and charge transport and by reducing the band gap of the polymer so that a larger fraction of the solar spectrum can be absorbed.

1. Introduction

As the evidence for global warming continues to build, it is becoming clear that we will have to find non-CO_2-releasing ways to create, transport, and store electricity. For photovoltaic (PV) cells to gain widespread acceptance as a source of clean and renewable energy, the cost per watt of solar energy must be decreased. Currently, the main barrier that prevents photovoltaic technology from providing a large fraction of our electricity is the high cost of manufacturing crystalline silicon. Although the cost per peak watt of crystalline silicon PV cells has dropped significantly over the past decade,[1] these PV cells are still too expensive to compete with conventional grid electricity without the benefit of government subsidies.[2] One potential alternative to crystalline silicon PV cells is cells made from thin films ($<1\ \mu$m) of conjugated (semiconducting) polymers, which can easily be cast onto flexible substrates over a large area using wet-processing techniques. These organic PV cells could provide electricity at a lower cost than crystalline silicon solar cells if a reasonable power efficiency (~10%) and lifetime (~10 years) could be achieved on a large scale. To reach these performance levels, however, several technological hurdles must be overcome. We begin this review with a discussion of the photovoltaic properties of organic semiconductors, including a general overview of the properties of these materials that make them attractive as candidates for use in PV cells, as well as their limitations. We next review the successive improvements that have been made in the device structure of conjugated polymer PV cells over the past decade to overcome these limitations. We then present what we believe to be the ideal device structure for conjugated polymer-based PV cells and describe some of the first efforts to make it. In the final section of this review we present an outlook for the future of conjugated polymer-based PV cells and discuss what must be done to maximize their efficiency.

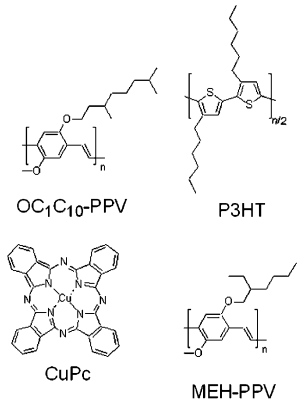

Figure 1. Chemical structures of four different organic semiconductors.

2. Conjugated Polymers for Photovoltaics

The chemical structures of four organic semiconductors commonly used in photovoltaic cells are shown in Figure 1. While films of copper phthalocyanine (CuPc) must generally be deposited by evaporation onto a substrate, the conjugated polymers poly(3-hexylthiophene) (P3HT), poly[2-methoxy-5-(2′-ethylhexoxy)-1,4-phenylenevinylene] (MEH-PPV), and poly[2-methoxy-5-(3′,7′-dimethyloctyloxy)-*p*-phenylenevinylene] (OC_1C_{10}-PPV) contain side chains that make them soluble in common organic solvents. This allows these polymers to be cast from solution using wet-processing techniques such as spin casting, dip coating,[3] ink jet printing,[4,5] screen printing,[6–8] and micromolding.[7] These techniques represent an enormously attractive route for producing large-area PV cells cheaply because they can be performed at ambient temperature and pressure, and because many of these techniques are scalable to large

* To whom correspondence should be addressed. Phone: (650) 736-0307, E-mail: mmcgehee@stanford.edu.

10.1021/cm049654n CCC: $27.50
Published on Web 00/00/0000 PAGE EST: 10

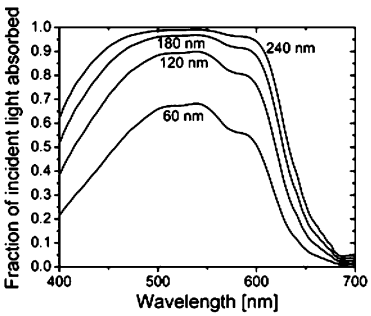

Figure 2. Fraction of incident light absorbed by P3HT as a function of wavelength for several different film thicknesses.

area with little material loss. Also, many of these techniques can be applied to systems that require flexible substrates,[9] such as roll-to-roll coaters.

A second major requirement for the active layer in a PV cell is that it should absorb a significant fraction of the sun's light. The high ($\sim 10^5$ cm^{-1}) peak optical absorption coefficient of many conjugated polymers makes them excellent candidates in this regard. While crystalline silicon PV cells must be made $\sim 100\ \mu$m thick to effectively absorb incident light, organic semiconductors have a direct band gap and generally must only be 100−500 nm thick to absorb most of the light at their peak absorption wavelength. Figure 2 shows the fraction of incident light absorbed by P3HT as a function of wavelength for several different film thicknesses. At a P3HT film thickness of 240 nm, greater than 95% of the incident light is absorbed over the wavelength range 450−600 nm, neglecting reflective losses. However, Figure 2 also highlights one of the biggest existing hurdles to reaching high-efficiency PV cells with conjugated polymers: the band gap of these semiconductors is too large and the absorption bandwidth of these materials is too narrow to absorb a large fraction of the solar spectrum. While the photon flux of the AM1.5G solar spectrum peaks around 700 nm (1.8 eV), P3HT, MEH-PPV, and OC_1C_{10}-PPV absorb strongly only over the wavelength range 350−650 nm (3.5−1.9 eV). As a result of this mismatch between the absorption spectrum of the organic semiconductor and the solar spectrum, the 240 nm thick film of P3HT shown in Figure 2 absorbs only about 21% of the sun's photons. Although a semiconductor with a 1.9 eV band gap could still be used to make an efficient PV cell if an open-circuit voltage (V_{oc}) could be attained that is close to 1.9 V, thereby giving a high power efficiency (defined as the maximum power produced by a PV cell divided by the power of incident light) despite only converting a small fraction of the sun's photons to current, in practice this has proven difficult to achieve in a PV cell made from conjugated polymers. In these cells V_{oc} values typically range between 0.5 and 1.2 V for devices that have reasonable photocurrents (>1 mA/cm^2) under AM1.5G illumination.

3. PV Cells Made from Single Layers of Conjugated Polymers

Although it is possible to generate a built-in field in an inorganic semiconductor through the controlled placement of n- and p-type dopant atoms, it is difficult to controllably dope most conjugated polymers. As a result of this, conjugated polymers are usually made as pure as is practically possible and can effectively be considered to be intrinsic semiconductors. Generating built-in electric fields within a film in the dark requires sandwiching the polymer between electrodes with varying work functions or incorporating interfaces with a second semiconductor into the device structure.[10] In one of the first reported conjugated polymer PV cells,[11] a photovoltaic effect was observed in a device made by spin casting and thermally converting an undoped thin layer of PPV on top of a transparent indium−tin oxide (ITO) electrode and then evaporating on a low-work-function top contact, as shown schematically in Figure 3a. When light with ~ 10 mW/cm^2 intensity was shone on the PV cell, an open-circuit voltage between 1.2 and 1.7 V was produced, depending on the metal used. In most cases the open-circuit voltage was roughly equal to the difference in work function between the top and bottom electrodes divided by the charge of an electron. This showed that in single-layer conjugated polymer PV cells, the sign and magnitude of V_{oc} could at least be partially attributed to an electrode work-function difference. However, it must be added that further research has shown that there are several other important factors that contribute to V_{oc}, such as nonnegligible dark current,[12] Fermi level pinning,[13] and chemical potential gradients.[14,15]

Although single-layer PV cells tend to produce a reasonable V_{oc}, their photocurrent is typically very low. For example, at an excitation wavelength of 458 nm, the above ITO−PPV−metal device had only 0.1−1% external quantum efficiency (EQE, defined as the number of electrons produced by a PV cell for each incident photon).[11] The discrepancy between the large fraction of photons absorbed at the wavelength of maximum absorption by a ~ 100 nm thick conjugated polymer film (>50%) and the low EQE (1%) of single-layer PV cells reveals the strong tendency of photogenerated electrons and holes to recombine in conjugated polymers. There are two major causes for this phenomenon. First, while the exact nature of the interaction between the electron and hole in a conjugated polymer is still a subject of debate,[16] it is clear that the predominant tendency of these materials is to form bound excitons that decay rather than dissociate at room temperature.[14] Second, even when free carriers are created in conjugated polymers via charge injection or exciton dissociation at an interface, these carriers typically have very low mobilities. The disordered nature of these semiconductors causes the transport of carriers to occur through a hopping mechanism rather than through bandlike transport. Hole mobilities that have been reported for conjugated polymers range from 10^{-1} to 10^{-7} cm^2/(V s),[17−20] while electron mobilities are typically lower (10^{-4}−10^{-9} cm^2/(V s)[18,21]). By contrast, the hole and electron mobilities in crystalline silicon are 475 and 1500 cm^2/(V s).[22] With carrier mobilities in polymer semiconductors that are many orders of magnitude lower than their crystalline counterparts, recombinative carrier loss can occur in polymer PV cells even under short-circuit conditions. The wide range of reported carrier mobilities in conjugated polymers results primarily from extreme sensitivity of the mobility to the morphology of the polymer film. There is also evidence

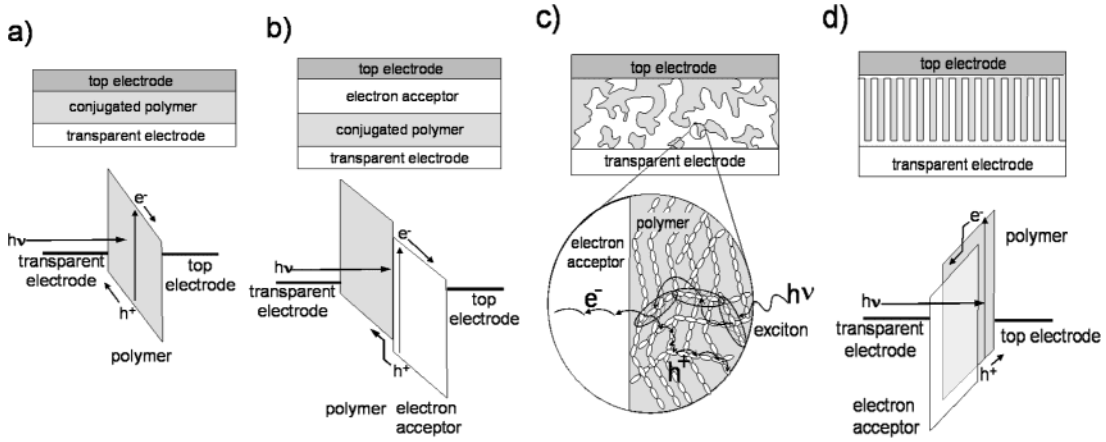

Figure 3. Four device architectures of conjugated polymer-based photovoltaic cells: (a) single-layer PV cell; (b) bilayer PV cell; (c) disordered bulk heterojunction; (d) ordered bulk heterojunction.

that the carrier mobility in conjugated polymers increases with carrier concentration.[23]

4. PV Cells Made from Two Layers of Organic Semiconductors

The phenomenon of exciton recombination and poor carrier transport in PV cells has also been observed in pure films of nonpolymeric organic semiconductors. One key improvement to the structure of PV cells made from these films was made by C. W. Tang in 1985 when he discovered that, by making two-layer PV cells with organic semiconductors that have offset energy bands, the external quantum efficiency of PV cells could be improved to 15% at the wavelength of maximum absorption.[24,25] By analyzing the shape of the EQE spectrum for his two-layer device, Tang deduced that the improved efficiency resulted from exciton dissociation at the interface between the two semiconductors. Excitons generated within a few nanometers of the heterojunction could diffuse to the interface and undergo forward electron or hole transfer, as depicted schematically in Figure 3b. This process of forward charge transfer led to the spatial separation of the electron and hole, thereby preventing direct recombination and allowing the transport of electrons to one electrode and holes to the other. Because there were essentially no minority free carriers in the undoped semiconductors, there was little chance of carrier recombination once the charges moved away from the interface, despite the long transit times to the electrodes.

Sariciftci et al. first applied this two-layer technique to a conjugated polymer PV cell by evaporating C_{60} on top of a spin-cast MEH-PPV layer.[26] In this cell the MEH-PPV was used to absorb visible light and transport holes to the ITO electrode following exciton dissociation at the interface. The C_{60}, with an electron affinity about 0.7 eV greater than that of MEH-PPV, was used to accept electrons from the conjugated polymer and transport them to the aluminum or gold top electrode. While the initially reported bilayer device produced ~1.2% EQE at 514 nm and showed only a slight improvement over pure polymer films, Halls et al. were able to subsequently obtain 9% EQE with the same materials by optimizing the thickness of the MEH-PPV and C_{60} layers.[27] These experiments demonstrated the concept that, for efficient PV cells to be made from conjugated polymers, an interface between the polymer and another semiconductor is necessary to allow excitons to dissociate. However, these experiments also revealed that, as in the organic PV cell made by Tang, the excitons in these materials need to be generated near the interface for dissociation to occur before recombination. The exciton diffusion length in several different conjugated polymers has subsequently been measured to be 4−20 nm.[27−31] Because the exciton diffusion length in a conjugated polymer is typically less than the absorption length of the material (~100 nm), the EQE of a bilayer device made with a conjugated polymer and another semiconductor is ultimately limited by the number of photons that can be absorbed within an exciton diffusion length of the interface.

More recently, there have been reports of PV cells made from bilayers of a conjugated polymer and TiO_2, which is a wide-band-gap (3.2 eV) inorganic semiconductor that accepts electrons from many organic semiconductors.[30,32,33] Savenjie et al. made the first such device by depositing a thin film of TiO_2 on a transparent ITO electrode using a sol−gel route and then spin casting MEH-PPV on top of the TiO_2.[30] In these cells, the electrons travel to the transparent bottom electrode and holes travel to the top electrode, which results in current flow in the opposite direction from polymer−C_{60} bilayer PV cells. A 1% EQE maximum and a 0.15% power efficiency under white light were measured. Arango et al. improved the efficiency of conjugated polymer−TiO_2 bilayer PV cells by using a phenylamino-*p*-phenylenevinylene derivative (PA-PPV) instead of MEH-PPV.[34] Because of the improved hole mobility and exciton diffusion length in the PA-PPV, a 25% EQE was achieved at the absorption maximum of the polymer, which is very impressive considering the flat interface between the two layers. A monochromatic power efficiency of 3.9% was reported at a wavelength of 435 nm for this device.

5. Bulk Heterojunction Conjugated Polymer PV Cells

5.1. Polymer−Polymer PV Cells. To address the problem of limited exciton diffusion length in conjugated polymers, Yu et al.[35] and Halls et al.[36] independently intermixed two conjugated polymers with offset energy levels so that all excitons would be formed near an

interface, as depicted in Figure 3c. They observed that the photoluminescence from each of the polymers was quenched. This implied that the excitons generated on one polymer within the film reached an interface with the other polymer and dissociated before recombining. This device structure, called a bulk heterojunction, provided a route by which nearly all photogenerated excitons in the film could be split into free carriers. Photovoltaic cells made from these blends initially gave only ~6% EQE at low light intensity, but improvements arising from the optimization of the device morphology through a lamination technique and from a better choice of the electron- and hole-transporting polymers resulted in PV cells with 29% EQE at 500 nm and 1.9% power efficiency under the AM1.5 solar spectrum.[37]

5.2. Polymer−PCBM PV Cells. Shortly after it was discovered that a blend of two conjugated polymers with offset energy levels could be used to separate electrons and holes and prevent direct recombination in the polymers, Yu et al. found that, by blending MEH-PPV with a solublized form of C_{60} called (6,6)-phenyl C_{61}-butyric acid methyl ester (PCBM), both total luminescence quenching of the polymer and much better carrier transport could be achieved.[38] This resulted in a dramatic improvement in device performance, with external quantum efficiency reaching 45% under low-intensity light when 80 wt % PCBM was used. In these PV cells, both the electron-accepting PCBM and hole-transporting conjugated polymer are in contact with each electrode. Despite the fact that electrons and holes can reach both electrodes in this system, it is generally true that the electrons travel to the metal top electrode and holes travel to the transparent bottom electrode at short circuit. Although it is not yet fully understood whether the direction of the photocurrent and the sign and magnitude of V_{oc} result primarily from the built-in field across the device or from selective contacts that can remove only one carrier type effectively,[14] there have been three recent studies which have begun to elucidate the origins of V_{oc} in this system. One investigation by Frohne et al. has shown that the work function of the transparent bottom electrode strongly affects V_{oc}.[39] Another study, performed by Brabec et al., has shown that V_{oc} shows only a weak dependence on the work function of the evaporated metal top electrode,[13] which has led to the hypothesis that the Fermi level of the metal top electrode is pinned to the LUMO (lowest unoccupied molecular orbital) of PCBM molecules in the blended film. In a third study, Milhailetchi et al. observed that the Fermi level is only pinned at the cathode if the metal's work function is less than the electron affinity of PCBM.[40]

The conjugated polymer−PCBM bulk heterojunction is currently the best conjugated polymer-based PV cell. One significant improvement to this device structure was made recently by Shaheen et al.,[41] who found that the morphology of the blend could be optimized by casting the polymer and PCBM from a solvent that prevents long-range phase separation and enhances the polymer chain packing.[42] As shown in Figure 4, this prevented the formation of isolated regions of polymer and PCBM in the film and gave the polymer increased hole mobility,[43] resulting in a device with more than double the EQE of the previous best device and with

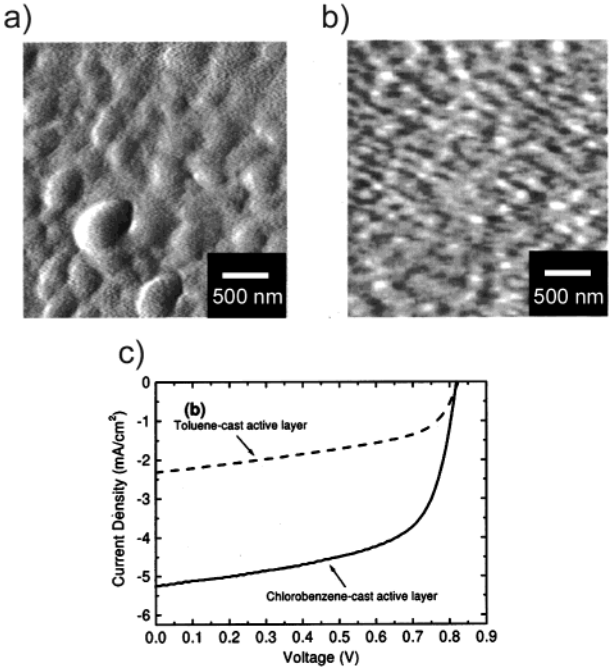

Figure 4. AFM images of the top surface of 100 nm films of DMO-PPV−PCBM blends after spin coating from (a) toluene and (b) chlorobenzene solutions, indicating phase separation on the order of 500 nm in (a) and less than 100 nm in (b). The $J-V$ curves under AM1.5 illumination for PV cells made using these solvents are shown in (c). (Reproduced from Ref. 41 with permission of the American Institute of Physics).

2.5% power efficiency under AM1.5G conditions. A second improvement came when it was found that switching the conjugated polymer from PPV derivatives to P3HT could give a further increase in hole mobility,[44] giving photovoltaic cells with EQE above 70% at the absorption maximum and 3.5% power efficiency under white light illumination.

Both of these advances in the polymer−PCBM PV cell highlight the need for device architectures that give optimized charge separation and charge transport in the two phases of a bulk heterojunction. If a high degree (>95%) of exciton dissociation can be guaranteed in the PV cell by intermixing the two phases well enough, as is generally the case in the polymer−PCBM PV cell because of the high cosolubility of the two constituents, then achieving high external quantum efficiency will result from extracting the separated carriers from the film before the competing process of interfacial recombination can occur. This recombination process, called back electron transfer, occurs when a hole on the conjugated polymer recombines with an electron on the electron-accepting material. For the OC_1C_{10}-PPV−PCBM system, this process typically occurs in the first 1−10 μs following exciton dissociation, although a small fraction of the excitations are long-lived and require milliseconds to recombine.[45,46] In conjugated polymer−PCBM films thicker than 100 nm, this recombination rate becomes competitive with the transport time for carriers to reach the electrodes, resulting in recombinative loss rather than increased external current. Because PCBM does not absorb strongly and an 80% weight fraction of PCBM is required to optimize transport properties, a PV cell with an optimal film thickness of 100 nm is ultimately limited by the ability of the film

to absorb light. Forexample, in the case of a 100 nm film of 20 wt % OC_1C_{10}-PPV and 80 wt % PCBM, only slightly more than half of the incident photons are absorbed at the wavelength of maximum absorption.[41] To achieve improved light absorption using films with an optimal film thickness of several hundred nanometers, it will be necessary to reduce the transport time for carriers to reach the electrodes. Recent studies of the transport through these films have indicated that the holes in the conjugated polymer are less mobile than the electrons in PCBM, so that it is hole transport which is competitive with back recombination.[47−50] These findings seem to have overturned the traditional belief that the device performance in polymer−PCBM PV cells is limited by electron hopping between PCBM molecules and suggest that improved hole mobility will be required to give higher EQE in these cells.

5.3. Conjugated Polymer−CdSe Nanocrystal Bulk Heterojunction PV Cells. A third type of bulk heterojunction that has achieved impressive efficiency is the conjugated polymer−CdSe nanocrystal PV cell. This PV cell has an architecture that is similar to that of the polymer−PCBM PV cell, except that the PCBM molecules are replaced by nanocrystals of CdSe. Using CdSe nanocrystals offers the advantage of having two components in the bulk heterojunction that can absorb visible light (the band edge of bulk CdSe is around 720 nm) and contribute to the photocurrent. In addition, the shape of the CdSe nanocrystals can be controlled to give highly elongated molecules, resulting in better pathways for electron transport.

The first experiments involving blends of conjugated polymers and inorganic nanocrystals came in 1996, when Greenham et al. reported PL quenching in MEH-PPV after intermixing it with 5 nm diameter spherical CdS and CdSe nanoparticles.[51] To obtain PL quenching in excess of 95% in these blends, the authors found it necessary to remove the organic ligand trioctylphosphine oxide (TOPO) from the surface of the nanoparticles and replace it with pyridine. PL quenching in excess of 98% was observed when 90 wt % 5 nm diameter CdSe nanoparticles were blended with the MEH-PPV. However, in blends with lower weight fractions of the nanoparticles incomplete quenching was observed. TEM images revealed that phase separation in the blends was the primary cause for the incomplete quenching. Photovoltaic cells made by depositing these blended films on a transparent ITO electrode and using an evaporated aluminum top electrode produced 12% EQE under low-intensity light, and a power efficiency estimated to be around 0.1% under AM1.5G conditions. The device performance improved as the weight fraction of nanocrystals was increased, leading the authors to conclude that electron transport was the limiting process in photovoltaic conversion. In a subsequent report, Ginger and Greenham showed that the ability of the CdSe nanoparticles to quench the PL in conjugated polymers depended on the side chain structure of the polymer.[52] Polymers with side chains attached to both sides of the conjugated main chain showed much less PL quenching than polymers with side chains on one side only.

The next improvement in conjugated polymer−CdSe nanocrystal PV cells came in 1999, when Huynh et al.

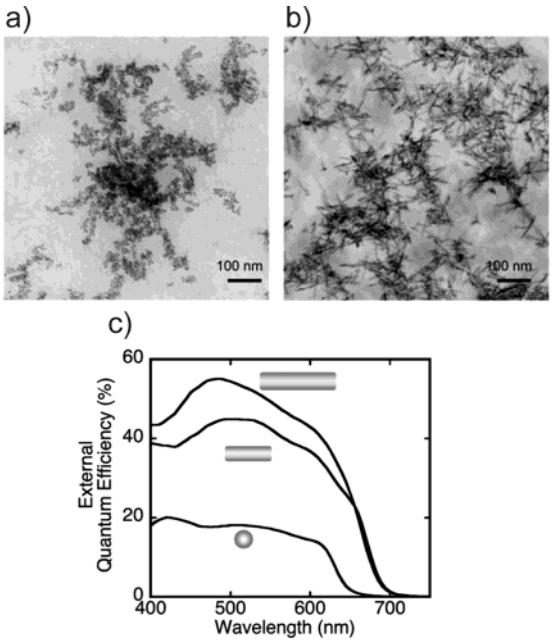

Figure 5. TEM images of P3HT−20 wt % CdSe nanocrystal blends. In (a) the nanocrystals are 7 nm by 7 nm; in (b) they are 7 nm by 60 nm. Part c shows the improved spectral response of devices made from P3HT−90 wt % CdSe nanocrystal blends as the nanocrystal length is increased from 7 to 30 to 60 nm. (Reproduced from Ref. 54 with permission of the American Association for the Advancement of Science).

discovered that electron transport in the film could be improved by using larger, slightly elongated nanocrystals that could pack efficiently within the film.[53] The authors also found that better hole transport could be obtained using P3HT instead of MEH-PPV. These changes in device structure produced 16% EQE under 0.48 mW/cm^2 514 nm illumination and increased the device fill factor to 0.5. The concept of using elongated nanocrystals to give improved electron transport was extended in 2002,[54] when a method was discovered for making well-blended films of P3HT and CdSe nanorods with high aspect ratios from a mixture of chloroform and pyridine.[55] With this technique it became possible to blend CdSe nanorods as long as 60 nm into P3HT, resulting in much better connectivity between nanorods than between spherical nanoparticles, as shown in the TEM images in Figure 5. This resulted in dramatically improved electron transport and increased the optimized film thickness to around 200 nm. Figure 5 also shows the spectral response of devices made with nanorods of increasing length. The highest EQE (55%) was achieved with the longest nanorods. This device produced 1.7% power efficiency under AM1.5G illumination. As in the case of the polymer−PCBM system, it is now believed that hole transport limits the device performance in the P3HT−CdSe nanorod system.[56] From the shape of the EQE spectrum shown in Figure 5, it can be deduced that both the CdSe nanorods and the P3HT contribute to the photocurrent in these devices, thereby extending the edge of the spectral response to 720 nm.

The most recent research on conjugated polymer−CdSe nanocrystal PV cells has focused on multidirectional growth of the nanocrystals.[57] By using branched CdSe nanocrystals that have four limbs extending

tetragonally away from a center linkage point (referred to as tetrapods), Sun et al. have been able to blend conjugated polymers with nanocrystals that extend partially perpendicular to the substrate rather than lying parallel to it, because of the three-dimensional shape of the branched nanoparticles.[58] Devices made with an 86% weight fraction of tetrapods blended with OC_1C_{10}-PPV showed 45% EQE at 480 nm, approximately double the EQE of a device made with the same weight fraction of 65 nm long nanorods. The tetrapod device showed 1.8% power efficiency under AM1.5G conditions.

5.4. Polymer−Titania PV Cells. A fourth type of bulk heterojunction PV cell that has recently received attention is the conjugated polymer−titania (TiO_2) PV cell. Although TiO_2 does not absorb visible light like CdSe, it does have some potential advantages over CdSe and PCBM as an electron-accepting material. The most attractive aspect of using TiO_2 with a conjugated polymer in a PV cell is the fact that the TiO_2 can be patterned into a continuous network for electron transport.[59,60] A continuous network for electron transport should allow a fairly high volume fraction of the conjugated polymer to be used in films, as long as the TiO_2 and polymer can be structured so that excitons can be dissociated effectively. Other reasons to use TiO_2 are that it is nontoxic, many molecules can be attached to its surface, and it has been used to make dye-sensitized solar cells with up to 10% power efficiency.[61−63]

At present, almost all of the work on conjugated polymer−TiO_2 PV cells has involved sintering together TiO_2 nanocrystals and then attempting to fill in the pores of the nanocrystalline film with a conjugated polymer, although there has also been one recent study involving films made by casting solutions that contained the polymer and a titania precursor.[64] The method of making a thin nanoporous TiO_2 film and then filling it in with conjugated polymer has the advantage of producing two truly bicontinuous phases in the PV cell. In addition, in a bulk heterojunction that is made by depositing the electron acceptor and conjugated polymer separately, it is much easier to prevent holes from reaching the negative electrode and electrons from reaching the positive electrode, thus preventing carriers from going to the wrong electrode. In PV cells made from conjugated polymers and TiO_2, it is generally the case that electrons are transported to the transparent bottom electrode because that is the electrode that the TiO_2 is connected to; similarly, holes are transported to the top electrode.[65,66] In these cells it is advantageous to use a high-work-function metal such as gold as the top electrode to provide an ohmic contact to the HOMO (highest occupied molecular orbital) of the polymer.

Arango et al. made the first polymer−TiO_2 bulk heterojunction PV cell by sintering together titania nanocrystals and then spin casting MEH-PPV on top.[65,67] A gold top electrode was used to extract holes from the polymer. For comparison the authors made bilayer PV cells with solid TiO_2 instead of nanoporous titania. They found that the EQE at the peak absorption wavelength of the polymer was 2% and 6% for the devices with solid and nanoporous TiO_2, respectively. They attributed the enhancement that arises in devices made from nanoporous titania to the increased interfacial area between the two semiconductors for exciton splitting. However, given the large fraction (>50%) of incident light that was absorbed in the device at the wavelength of maximum absorption of MEH-PPV, the fact that the EQE in the nanoporous devices only reached 6% indicates that incomplete pore filling was achieved by spin coating, that excitons in the pores were not split prior to geminate recombination, or that charge carriers were not able to escape the region of interpenetrating titania and polymer prior to back electron transfer. There have also been several studies of PV cells made with nanocrystalline TiO_2 and polythiophene derivatives.[68−73] In some cases a ruthenium dye was attached to the TiO_2 before the polymer was infiltrated into the pores. In the best devices made with these materials, Gebeyehu et al. observed energy conversion efficiencies as high as 0.16% under simulated solar irradiation.[68] A recent study by Ravirajan et al. using polyfluorene derivatives and thin (100 nm) layers of nanocrystalline TiO_2 produced 14% EQE at low light intensity and 0.16% power efficiency under AM1.5G conditions.[66]

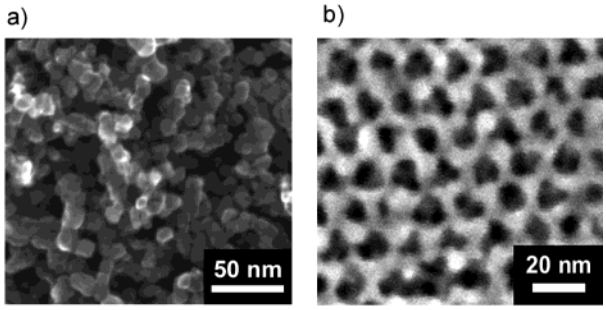

Figure 6. Top-view SEM images of (a) sintered TiO_2 nanocrystals and (b) mesoporous TiO_2.

External quantum efficiencies below 15% have been reported in nearly all of the reported bulk heterojunction PV cells made from nanocrystalline TiO_2 and conjugated polymers. Unfortunately, it is difficult to analyze the loss mechanisms in these PV cells quantitatively because there have been few reports that have determined how fully the conjugated polymer is infiltrated into the TiO_2 matrix, and without this knowledge it is impossible to calculate what the maximum EQE could be for a given exciton diffusion length in the polymer and infiltration depth into the TiO_2. However, on the basis of the SEM image of nanocrystalline TiO_2 shown in Figure 6, we can at least qualitatively identify one major loss mechanism in these films: There are too many large (50−100 nm) domains of empty space in nanocrystalline TiO_2 to give sufficient PL quenching of most conjugated polymers after the polymer has been infiltrated into the TiO_2.

6. Ideal Conjugated Polymer PV Cell Device Architecture

In all of the bulk heterojunction devices that we have described to this point, the conjugated polymer and electron acceptor have been randomly interspersed throughout the film. In the case of polymer−PCBM and polymer−CdSe nanorod devices, the random distribution of electron acceptors can lead to electron trapping on isolated acceptors unless a large weight fraction of acceptors is used. In both the polymer−CdSe and

polymer−nanoporous TiO_2 devices, the randomly distributed interface between the two semiconductors can lead to incomplete PL quenching in the conjugated polymer in regions of the polymer that are more than an exciton diffusion length away from an acceptor. For these reasons, some have sought to create well-ordered conjugated polymer−electron acceptor films. In an ideal device structure, as shown schematically in Figure 3d, every exciton formed on the conjugated polymer will be within a diffusion length of an electron acceptor, although quantitative modeling has pointed out that some light emission will still occur in the polymer even if this is the case.[74] Additionally, in the ideal structure both the conjugated polymer and electron acceptor should have straight pathways to the electrode to minimize the carrier transport time and reduce the probability of back electron transfer. A second strategy for reducing the probability of back electron transfer is to modify the interface between the two semiconductors, as has been done successfully in dye-sensitized solar cells.[75,76] We also believe that an ideal structure should be designed so that each phase of the bulk heterojunction is only in contact with one of the electrodes, which would help ensure a high shunt resistance through the device and prevent carrier loss at the wrong electrodes, although to some extent this requirement can be mitigated through the use of highly selective contacts.

Our group recently reported on first attempts at making ordered bulk heterojunctions using conjugated polymers and mesostructured TiO_2. We first fabricated well-ordered TiO_2 films with 8 nm pores using the block copolymer synthesis route developed by Alberius-Henning et al.[60] A high-resolution SEM top-view image of a film made with this method is shown in Figure 6. Although the pores in this film are not perfectly ordered, the pore size is highly uniform, which is desirable for the efficient dissociation of excitons. Films made using this synthesis route have pores that form an interconnected network within the film, but it should be emphasized that these films do not have pores that go straight to the bottom of the film. We have shown that P3HT can be infiltrated into the pores of mesoporous TiO_2 very effectively by spinning a film of the polymer on top of the mesoporous film and then heating the sample to infiltrate the polymer.[77] We measured the degree of polymer infiltration into the 50−300 nm mesoporous TiO_2 films using an X-ray photoelectron spectroscopy (XPS) depth profiling technique and found that the polymer chains could be infiltrated to the bottom of the TiO_2 film after heating at 200 °C for a few minutes. Because the pore size in these films is smaller than the radius of gyration of the polymer chain and it is likely that the polymer undergoes a conformational entropy loss as it is infiltrated into the pores, we hypothesize that a favorable enthalpic interaction between the polymer chain and the TiO_2 surface drives the infiltration. Interestingly, despite the fact that the pore size in these films was only 8 nm, we did not observe full PL quenching in the infiltrated P3HT depending on the infiltration conditions used (Figure 7a). As shown in Figure 7, both the absorption and photoluminescence spectra of the polymer in the pores following different infiltration conditions show a blue shift compared to the spectra of a neat film of P3HT.

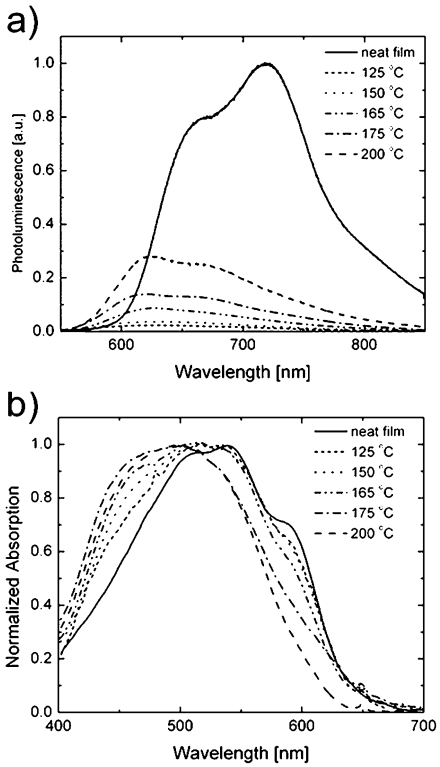

Figure 7. (a) Photoluminescence and (b) absorption spectra of P3HT in the pores of mesoporous TiO_2 following infiltration of the polymer at different temperatures. The spectra of a neat film of P3HT are included for comparison. All spectra were recorded at room temperature. (Republication with permission of Wiley-VCH).

This suggests that the polymer chains are twisted and not π-stacked on each other. At this point it is unclear whether the incomplete quenching resulted from reduced exciton mobility on the poorly packed infiltrated polymer chains, or from the pore size simply being too large given the small exciton diffusion length that has been observed in thiophene-based polymers.[29]

We have also reported on the photovoltaic properties of bulk heterojunctions made with mesoporous TiO_2 and P3HT, using SnO_2:F and silver as the bottom and top electrodes.[78] In the optimized device geometry with the polymer chains infiltrated approximately 20−30 nm into the mesoporous TiO_2 film, we obtained 10% EQE under 514 nm illumination, a factor of 3 improvement in EQE over devices made with nonporous TiO_2 (Figure 8). We estimated that the power efficiency of an optimized PV cell would be 0.45% under AM1.5G illumination by integrating the EQE spectrum of the device. We also found that the EQE of cells made from these materials dropped if the conjugated polymer was infiltrated more deeply than 20−30 nm into the mesopores. This indicates that holes generated on P3HT chains infiltrated deeply into the TiO_2 cannot escape from the film before undergoing back recombination, and that the hole mobility on the infiltrated P3HT chains limits the device performance. This is perhaps not too surprising given the fact that the P3HT chains take a highly nonlinear infiltration pathway to the bottom of the film. This conclusion is also corroborated by the spectral data presented in Figure 7**,** which indicate that the polymer chains are unable to π-stack in the strongly confining pores of the TiO_2. We believe that straight pores and

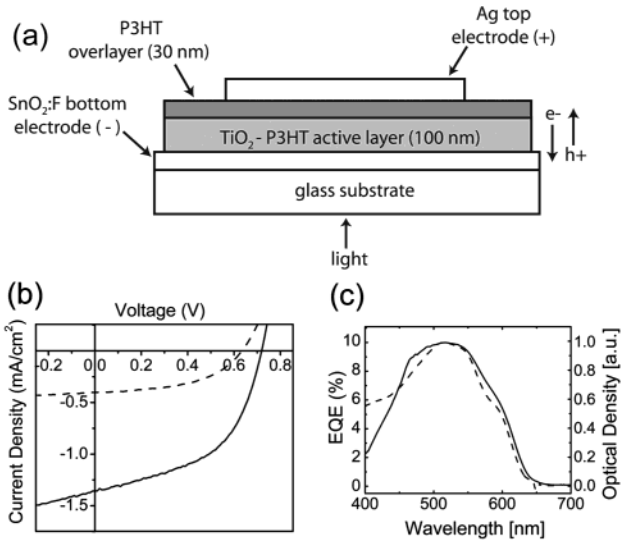

Figure 8. (a) Device structure, (b) $J-V$ curves under 33 mW/cm^2 514 nm illumination (solid curve), and (c) spectral response of a P3HT−mesoporous TiO_2 PV cell. In (b), the $J-V$ curve of a device made with nonporous TiO_2 rather than mesoporous TiO_2 is also shown (dotted curve). (Republication with permission of the American Institute of Physics).

perhaps a larger pore diameter will be required to give good hole transport in these films, and that this will lead to improved EQE.

We anticipate the development of several new research efforts soon that will attempt to improve the efficiency of conjugated polymer PV cells by using better ordered bulk heterojunctions, with some efforts already under way.[79,80] Implicit in this discussion of the ideal design for a conjugated polymer PV cell is the assumption that the materials needed for this design can actually be fabricated. Fortunately, there have been many exciting developments over the past several years concerning new methods of producing materials that are ordered on the nanometer length scale, such as the growth of silicon, GaAs, and ZnO nanowires and CdSe nanoparticles and nanorods and the fabrication of well-ordered mesoporous TiO_2 and SnO_2 films.[79,81−83] Much of the work on improving conjugated polymer PV cells over the next several years will undoubtedly involve an attempt to fabricate nanostructured materials that have the ideal geometry for exciton dissociation from the polymer, while simultaneously giving improved carrier transport in both components of the bulk heterojunction.

7. Prospects for High-Efficiency (10%) Conjugated Polymer Photovoltaic Cells

Since the discovery of the bulk heterojunction in 1995, tremendous progress has been made in improving the efficiency of conjugated polymer-based PV cells, with the best reported cell now producing above 70% EQE and ∼3.5% power efficiency.[44] Given the 100-fold lower power efficiencies that were produced in the first conjugated polymer PV cells a decade ago, a factor of 2.8 improvement to get to 10% efficiency seems almost trivial. However, some quantitative analysis of the situation shows that reaching this milestone will require significant innovation and effort, as we discuss in this section.

In the near term, it is likely that research efforts will continue to be focused on improving carrier transport in the two phases of the heterojunction, with the ultimate goal of producing PV cells with EQE greater than 90% across the wavelength range that is strongly absorbed by the polymer (450−600 nm). This will require the fabrication of PV cells that are either thicker or more light absorbent than currently optimized cells. For example, we can see from Figure 2 that, in PV cells made with P3HT as the absorbing material, a 240 nm film thickness of P3HT will be required to absorb enough light to make accomplishing this EQE possible, neglecting a possible enhancement in absorption that can occur if a reflecting back contact is used. If the light-absorbing capabilities of the film are reduced by the addition of transparent or weakly absorbing electron acceptors, then an even thicker film will be required. This is one area in which we believe the use of ordered bulk heterojunctions might be very useful, because in a bulk heterojunction with straight conduction pathways the transport time to the electrodes should be reduced, thereby allowing a thicker film to be used for a given back recombination lifetime. In addition, in an ordered bulk heterojunction it might be possible to use a smaller weight fraction of the electron-accepting material in the film, thus improving the light absorption in the film for a given film thickness. A second route to achieving higher EQE in conjugated polymer PV cells is through the development of polymers with higher carrier mobilities. As mentioned previously, it now appears that hole transport in the conjugated polymer is the limiting process in most bulk heterojunction polymer PV cells. For example, while the electron mobility of PCBM in an 80 wt % PCBM−OC_1C_{10}-PPV blend has been shown to be $(2-4) \times 10^{-3}$ cm^2/(V s),[48,49] the hole mobilities of OC_1C_{10}-PPV and of a polyfluorene-based conjugated polymer have both been found to be only $\sim 2 \times 10^{-6}$ cm^2/(V s) in blends of the same concentration.[47,48] Simple models developed by us and others[84] estimate that, for a 1 μs back recombination time constant and hole-limited transport, a hole mobility of $10^{-3}-10^{-2}$ cm^2/(V s) is required to result in an EQE greater than 90% across the wavelength range that is strongly absorbed by the polymer. Given that mobilities of 0.1 cm^2/(V s) have been achieved in polymer field effect transistors, it seems promising that higher hole mobilities can be achieved in PV cells.

In the long term, however, it is clear that, in addition to achieving idealized morphology and transport in these cells, some more fundamental improvements to the components of the bulk heterojunction will need to be made to reach 10% efficiency. In the P3HT−PCBM system, for example, it will not be possible to reach 10% power efficiency by simply improving the EQE of current devices, which is already 70%. Using a simple calculation that assumes 100% EQE for all photon energies above the 1.9 eV band gap of P3HT, the best possible P3HT−PCBM PV cell would produce roughly 17 mA/cm^2 of photocurrent under AM1.5G illumination. Combined with the open-circuit voltage (550 mV) and fill factor (0.6) that has been reported for this bulk heterojunction,[44] the resultant power efficiency would be only 5.6%. Thus, it is clear that, for the P3HT−PCBM PV cell to reach 10% efficiency, significant improvements

to the device fill factor and open-circuit voltage will need to be made, and this will require new device designs that give reduced recombination under forward bias.

In terms of the basic properties of the materials used in a bulk heterojunction, one area of research which should be pursued for conjugated polymer-based PV cells to reach high efficiency is the development of conjugated polymers and electron acceptors with lower band gaps than conventional P3HT, OC_1C_{10}-PPV, or nanocrystals of CdSe.[85,86] As mentioned previously, the thickest P3HT film shown in Figure 2 absorbs only about 21% of the sun's photons. If the absorption band of a conjugated polymer or a polymer−electron acceptor blend could be extended to the range 350−900 nm (3.5−1.4 eV) using new chemical syntheses of these materials, 46% of the sun's photons could be harnessed. This would effectively double the power efficiency of the best bulk heterojunction PV cells if the open-circuit voltage and fill factor of the cell are not adversely affected by the decreased band gap. This can be ensured to some extent by maintaining a constant energy difference between the HOMO of the polymer and the LUMO of the electron acceptor as one of their band gaps is decreased.

A second area where there is also room for improvement is reducing the energy loss that occurs during electron transfer. In the P3HT−TiO_2 system, for example, approximately 1 eV of energy is lost when electrons transfer from the polymer to the TiO_2. Figure 9 shows the maximum theoretical efficiency that can be achieved as a function of the band gap of a conjugated polymer when electrons lose 1 eV of energy during electron transfer to an electron acceptor. This plot was generated by assuming AM1.5G illumination, 100% EQE for photon energies above the band gap of the single light-absorbing polymer, a fill factor equal to 1, and an open-circuit voltage equal to the energy difference between the LUMO of the acceptor and the HOMO of the conjugated polymer. This simple calculation does not consider the reduction in these quantities that must occur in any real device as a result of the presence of a nonnegligible dark current.[87] Although it is not yet clear how the effect of the dark current can best be accounted for in a bulk heterojunction organic PV cell, it must be emphasized that an inclusion of this effect in our calculations would result in significantly lower theoretical maximum efficiencies than the ones shown here. While the maximum theoretical efficiency for a single 1.9 eV band gap absorber is 32%, the introduction of an electron acceptor with a 1 eV LUMO offset causes the maximum theoretical efficiency to decrease to 15%. Assuming more realistic values for the EQE, fill factor, and open-circuit voltage that account for reflective losses and recombinative losses suggests that it will be very difficult to reach 10% efficiency with these two materials. The concept of the deleterious effect of too much energy loss during forward electron transfer is extended in part b of Figure 9, which plots the maximum theoretical efficiency of a PV cell with an *optimal* band gap for a given LUMO offset versus the value of the offset. These simple calculations make it clear that, for the highest efficiency to be reached in bulk heterojunction PV cells, the energy band offset between the conjugated polymer and electron acceptor will need to be minimized while still allowing forward electron transfer to occur at a sufficiently high rate. This optimization will require the synthesis of both new conjugated polymers and new electron acceptors. On this front one recent report involving a 1.6 eV band gap conjugated polymer that shows electron transfer to PCBM despite only a ∼0.3 eV LUMO offset is encouraging.[86]

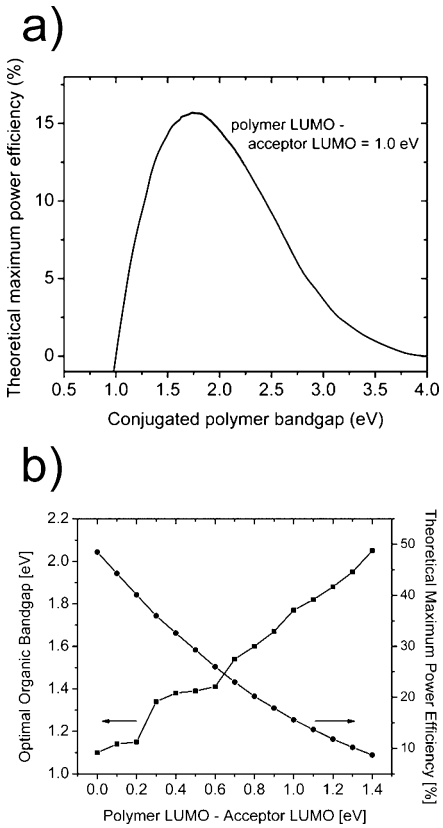

Figure 9. (a) Theoretical maximum power efficiency of a conjugated polymer−electron acceptor PV cell as a function of the polymer band gap when 1 eV of energy is lost during electron transfer. (b) Optimal polymer band gap and theoretical maximum power efficiency as a function of the energy loss during electron transfer. The effect of the dark current on the theoretical maximum efficiency is not included in the calculations used to generate these plots.

On the positive side of these calculations is the fact that, if improved materials and device architectures can be fabricated, there is no theoretical reason that will prevent conjugated polymer PV cells from producing efficiencies that are competitive with commercially produced crystalline silicon PV cells. Reaching 10−20% efficiency will come partially from better designed organic PV cell architectures, but it will also require the synthesis of new conjugated polymers with smaller band gaps, wider bandwidths, optimized energy levels, and higher carrier mobilities. It is these innovations that will be the key to allowing plastic solar cells to become a viable energy source for the 21st century.

Acknowledgment. We acknowledge the Camille and Henry Dreyfus Foundation, the Petroleum Research Fund, and the Stanford Office of Technology Licensing for funding our research at Stanford. We thank Yuxiang Liu, Sean Shaheen, and Brian Gregg for helpful conversations.

References

(1) Shah, A.; Torres, P.; Tscharner, R.; Wyrsch, N.; Keppner, H. *Science* **1999**, *285*, 692.
(2) Johnson, J. C. *Chem. Eng. News* **2004**, *82*, 25.
(3) Wang, G.; Swenson, J.; Moses, D.; Heeger, A. J. *J. Appl. Phys.* **2003**, *93*, 6137.
(4) Hebner, T. R.; Wu, C. C.; Marcy, D.; Lu, M. H.; Sturm, J. *Appl. Phys. Lett.* **1998**, *72*, 519.
(5) Chang, S.; Liu, J.; Bharathan, J.; Yang, Y.; Onohara, J.; Kido, J. *Adv. Mater.* **1999**, *11*, 734.
(6) Pschenitzha, F.; Sturm, J. C. *Appl. Phys. Lett.* **1999**, *74*, 1913.
(7) Rogers, J. A.; Bao, Z.; Raju, V. R. *Appl. Phys. Lett.* **1998**, *72*, 2716.
(8) Shaheen, S. E.; Radspinner, R.; Peyghambarian, N.; Jabbour, G. E. *Appl. Phys. Lett.* **2001**, 2996.
(9) Gustafsson, G.; Cao, Y.; Treacy, G. M.; Klavetter, F.; Colaneri, N.; Heeger, A. J. *Nature* **1992**, *357*, 477.
(10) Parker, I. D. *J. Appl. Phys.* **1994**, *75*, 1656.
(11) Marks, R. N.; Halls, J. J. M.; Bradley, D. D. C.; Friend, R. H.; Homes, A. B. *J. Phys.: Condens. Matter* **1994**, *6*, 1379.
(12) Malliaras, G. G.; Salem, J. R.; Brock, P. J.; Scott, J. C. *J. Appl. Phys.* **1998**, *84*, 1583.
(13) Brabec, C. J.; Cravino, A.; Meissner, D.; Sariciftci, N. S.; Fromherz, T.; Rispens, M. T.; Sanchez, L.; Hummelen, J. C. *Adv. Funct. Mater.* **2001**, *11*, 374.
(14) Gregg, B. A. *J. Phys. Chem. B* **2003**, *107*, 4688.
(15) Ramsdale, C. M.; Barker, J. A.; Arias, A. C.; Mackenzie, J. D.; R. H. Friend, Greenham, N. C. *J. Appl. Phys.* **2002**, *92*, 4266.
(16) Sariciftci, N. S. *Primary Photoexcitations in Conjugated Polymers*; World Scientific Publishing Co.: Singapore, 1998.
(17) Bao, Z.; Dodabalapur, A.; Lovinger, A. *Appl. Phys. Lett.* **1996**, *69*, 4108.
(18) Bozano, L.; Carter, S. A.; Scott, J. C.; Malliaras, G. G.; Brock, P. J. *Appl. Phys. Lett.* **1999**, *74*, 1132.
(19) Kline, R. J.; Mcgehee, M. D.; Kadnikova, E. N.; Liu, J.; Frechet, J. M. J. *Adv. Mater.* **2003**, *15*, 1519.
(20) Sirringhaus, H.; Tessler, N.; Friend, R. *Science* **1998**, *280*, 1741.
(21) Babel, A.; Jenekhe, S. *Adv. Mater.* **2002**, *14*, 371.
(22) Sze, S. M. *VLSI Technology*, 2nd ed.; McGraw-Hill Publishing Co.: New York, 1988.
(23) Tanase, C.; Meijer, E. J.; Blom, P. W. M.; De Leeuw, D. M. *Phys. Rev. Lett.* **2003**, *91*, 216601.
(24) Tang, C. W. *Appl. Phys. Lett.* **1986**, *48*, 183.
(25) Peumans, P.; Yakimov, A.; Forrest, S. *J. Appl. Phys.* **2003**, *93*, 3693.
(26) Sariciftci, N. D.; Braun, D.; Zhang, C.; Srdanov, V. I.; Heeger, A. J.; Stucky, G.; Wudl, F. *Appl. Phys. Lett.* **1993**, *62*, 585.
(27) Halls, J. M.; Pichler, K.; Friend, R. H.; Moratti, S. C.; Holmes, A. B. *Appl. Phys. Lett.* **1996**, *68*, 3120.
(28) Pettersson, L. A. A.; Roman, L. S.; Inganas, O. *J. Appl. Phys.* **1999**, *86*, 487.
(29) Theander, M.; Yartsev, A.; Zigmantas, D.; Sundström, V.; Mammo, W.; Anderson, M. R.; Inganäs, O. *Phys. Rev. B* **2000**, *61*, 12957.
(30) Savenije, T. J.; Warman, J. M.; Goossens, A. *Chem. Phys. Lett.* **1998**, *287*, 148.
(31) Haugeneder, A.; Neges, M.; Kallinger, C.; Spirkl, W.; Lemmer, U.; Feldman, J.; Scherf, U.; Harth, E.; Gugel, A.; Mullen, K. *Phys. Rev. B* **1999**, *59*, 15346.
(32) Van Hal, P. A.; Christiaans, M. P. T.; Wienk, M. M.; Kroon, J. M.; Janssen, R. A. J. *J. Phys. Chem. B* **1999**, *103*, 4352.
(33) Anderson, N. A.; Hao, E.; Ai, X.; Hastings, G.; Lian, T. *Chem. Phys. Lett.* **2001**, *347*, 304.
(34) Arango, A. C.; Johnson, L. R.; Bliznyuk, V. N.; Schlesinger, Z.; Carter, S.; Hörhold, H. H. *Adv. Mater.* **2000**, *12*, 1689.
(35) Yu, G.; Heeger, A. J. *J. Appl. Phys.* **1995**, *78*, 4510.
(36) Halls, J. J. M.; Walsh, C. A.; Greenham, N. C.; Marseglia, E. A.; Friend, R. H.; Moratti, S. C.; Holmes, A. B. *Nature* **1995**, *376*, 498.
(37) Granstrom, M.; Petritsch, K.; Arias, A. C.; Lux, A.; Andersson, M. R.; Friend, R. H. *Nature* **1998**, *395*, 257.
(38) Yu, G.; Gao, J.; Hummelen, J. C.; Wudl, F.; Heeger, A. J. *Science* **1995**, *270*, 1789.
(39) Frohne, H.; Shaheen, S. E.; Brabec, C. J.; Muller, D. C.; Sariciftci, N. S.; Meerholz, K. *ChemPhysChem* **2002**, *3*, 795.
(40) Mihailetchi, V. D.; Blom, P. W. M.; Hummelen, J. C.; Rispens, M. T. *J. Appl. Phys.* **2003**, *94*, 6849.
(41) Shaheen, S. E.; Brabec, C. J.; Sariciftci, N. S.; Padinger, F.; Fromherz, T.; Hummelen, J. C. *Appl. Phys. Lett.* **2001**, *78*, 841.
(42) Van Duren, J. K. J.; Yang, X.; Loos, J.; Bulle-Liewma, C. W. T.; Sieval, A. B.; Hummelen, J. C.; Janssen, R. A. J. *Adv. Funct. Mater.* **2004**, *14*, 425.
(43) Geens, W.; Shaheen, S. E.; Wessling, B.; Brabec, C. J.; Poortmans, J.; Sariciftci, N. S. *Org. Electron.* **2002**, *3*, 105.
(44) Padinger, F.; Rittberger, R. S.; Sariciftci, N. S. *Adv. Funct. Mater.* **2003**, *13*, 85.
(45) Nelson, J. *Phys. Rev. B* **2003**, *67*, 155209.
(46) Nogueira, A. F.; Montanari, I.; Nelson, J.; Durrant, J. R.; Winder, C.; Sariciftci, N. S.; Brabec, C. J. *J. Phys. Chem. B* **2003**, *107*, 1567.
(47) Choulis, S. A.; Nelson, J.; Kim, Y.; Poplavskyy, D.; Kreouzis, T.; Durrant, J. R.; Bradley, D. *Appl. Phys. Lett.* **2003**, *83*, 3812.
(48) Pacios, R.; Nelson, J.; Bradley, D.; Brabec, C. J. *Appl. Phys. Lett.* **2003**, *83*, 4764.
(49) Van Duren, J. K. J.; Mihailetchi, V. D.; Blom, P. W. M.; Van Woudenbergh, T.; Hummelen, J. C.; Rispens, M. T.; Janssen, R. A. J.; Wienk, M. M. *J. Appl. Phys.* **2003**, *94*, 4477.
(50) Mihailetchi, V. D.; Van Duren, J. K. J.; Blom, P. W. M.; Hummelen, J. C.; Janssen, R. A. J.; Kroon, J. M.; Rispens, M. T.; Verhees, W. J. H.; Wienk, M. M. *Adv. Funct. Mater.* **2003**, *13*, 43.
(51) Greenham, N. C.; Peng, X.; Alivisatos, A. P. *Phys. Rev. B* **1996**, *54*, 17628.
(52) Ginger, D. S.; Greenham, N. C. *Phys. Rev. B* **1999**, *59*, 10622.
(53) Huynh, W. U.; Peng, X.; Alivisatos, A. P. *Adv. Mater.* **1999**, *11*, 923.
(54) Huynh, W. U.; Dittmer, J. J.; Alivisatos, A. P. *Science* **2002**, *295*, 2425.
(55) Huynh, W. U.; Dittmer, J. J.; Libby, W. C.; Whitting, G. L.; Alivisatos, A. P. *Adv. Funcy. Mater.* **2003**, *13*, 73.
(56) Huynh, W. U.; Dittmer, J. J.; Teclemariam, N.; Milliron, D. J.; Alivisatos, A. P.; Barnham, K. W. J. *Phys. Rev. B* **2003**, *67*, 115326.
(57) Manna, L.; Milliron, D. J.; Meisel, A.; Scher, E. C.; Alivisatos, A. P. *Nat. Mater.* **2003**, *2*, 382.
(58) Sun, B. Q.; Marx, E.; Greenham, N. C. *Nano Lett.* **2003**, *3*, 961.
(59) Soler-Illia, G. J. D. A.; Louis, A.; Sanchez, C. *Chem. Mater.* **2002**, *14*, 750.
(60) Alberius-Henning, P.; Frindell, K. L.; Hayward, R. C.; Kramer, E. J.; Stucky, G. D.; Chmelka, B. F. *Chem. Mater.* **2002**, *14*, 3284.
(61) O'regan, B.; Gratzel, M. *Nature* **1991**, *353*, 737.
(62) Bach, U.; Lupo, D.; Comte, P.; Moser, J. E.; Weissortel, F.; Salbeck, J.; Spreitzer, H.; Gratzel, M. *Nature* **1998**, *395*, 583.
(63) Hagfelt, A.; Gratzel, M. *Acc. Chem. Res.* **2000**, *33*, 269.
(64) Van Hal, P. A.; Wienk, M. M.; Kroon, J. M.; Verhees, W. J. H.; Slooft, L. H.; Van Gennip, W. J. H.; Jonkheijm, P.; Janssen, R. A. J. *Adv. Mater.* **2003**, *15*, 118.
(65) Arango, A. C.; Carter, S. A.; Brock, P. J. *Appl. Phys. Lett.* **1999**, *74*, 1698.
(66) Ravirajan, P.; Haque, S. A.; Durrant, J. R.; Poplavskyy, D.; Bradley, D. D. C.; Nelson, J. *J. Appl. Phys.* **2004**, *95*, 1473.
(67) Breeze, A. J.; Schlesinger, Z.; Carter, S. A.; Brock, P. J. *Phys. Rev. B* **2001**, *64*, 1252051.
(68) Gebeyehu, D.; Brabec, C. J.; Sariciftci, N. S.; Vangeneugden, D.; Kiebooms, R.; Vanderzande, D.; Kienberger, F.; Schindler, H. *Synth. Met.* **2001**, *125*, 279.
(69) Gebeyehu, D.; Brabec, C. J.; Padinger, F.; Fromherz, T.; Spiekermann, S.; Vlachopoulos, N.; Kienberger, F.; Schindler, H.; Sariciftci, N. S. *Synth. Met.* **2001**, *121*, 1549.
(70) Gebeyehu, D.; Brabec, C. J.; Sariciftci, N. S. *Thin Solid Films* **2002**, *403*, 271.
(71) Luzzati, S.; Basso, M.; Catellani, M.; Brabec, C. J.; Gebeyehu, D.; Sariciftci, N. S. *Thin Solid Films* **2002**, *403*, 52.
(72) Spiekermann, S.; Smestad, G.; Kowalik, J.; Tolbert, L. M.; Gratzel, M. *Synth. Met.* **2001**, *121*, 1603.
(73) Huisman, C. L.; Goossens, A.; Schoonman, J. *Synth. Met.* **2003**, *138*, 237.
(74) Kannan, B.; Castelino, K.; Majumdar, A. *Nano Lett.* **2003**, *3*, 1729.
(75) Zaban, A.; Chen, S. G.; Chappel, S.; Gregg, B. A. *Chem. Commun.* **2000**, 2231.
(76) Palomares, E.; Clifford, J. N.; Haque, S. A.; Lutz, T.; Durrant, J. R. *Chem. Commun.* **2002**, 1464.
(77) Coakley, K. M.; L. Y., Mcgehee, M. D.; Frindell, K. M.; Stucky, G. D. *Adv. Funct. Mater.* **2003**, *13*, 301.
(78) Coakley, K. M.; Mcgehee, M. D. *Appl. Phys. Lett.* **2003**, *83*, 3380.
(79) Shaheen, S. E.; Ginley, D. S. *Encycl. Nanosci. Nanotechnol.* **2004**.
(80) Hadziiouannou, G. *MRS Bull.* **2002**, *27*, 456.
(81) Yang, P.; Zhao, D.; Margolese, D. I.; Chmelka, B. F.; Stucky, G. D. *Nature* **1998**, *396*, 152.
(82) Greene, L. E.; Law, M.; Goldberger, J.; Kim, F.; Johnson, J. C.; Zhang, Y.; Saykally, R. J.; Yang, P. *Angew. Chem., Int. Ed.* **2003**, *42*, 3021.
(83) Xia, Y.; Yang, P.; Sun, Y.; Wu, Y.; Mayers, B.; Gates, B.; Yin, Y.; Kim, F.; Yan, H. *Adv. Mater.* **2003**, *15*, 353.
(84) Brabec, C. J.; Shaheen, S. E.; Fromherz, T.; Padinger, F.; Hummelen, J.; Dhanabalan, A.; Janssen, R. A. J.; Sariciftci, N. S. *Synth. Met.* **2001**, *121*, 1517.
(85) Winder, C.; Sariciftci, N. S. *J. Mater. Chem.* **2004**, *14*, 1077.
(86) Brabec, C. J.; Winder, C.; Sariciftci, N. S.; Hummelen, J. C.; Dhanabalan, A.; Van Hal, P. A.; Janssen, R. A. J. *Adv. Funct. Mater.* **2002**, *12*, 709.
(87) Shockley, W.; Quessier, H. J. *J. Appl. Phys.* **1961**, *32*, 510.

CM049654N